Cerenkov luminescence imaging of medical isotopes

Alessandro Ruggiero,[a†] Jason P. Holland, [b†] Jason S. Lewis[b,c] and Jan Grimm [a,c*]

[a] Nuclear Medicine Service, Department of Radiology, Memorial Sloan-Kettering Cancer Center, 1275 York Avenue, New York, United States of America, NY10065.

[b] Radiochemistry Service, Department of Radiology, Memorial Sloan-Kettering Cancer Center, 1275 York Avenue, New York, United States of America, NY10065.

[c] Program in Molecular Pharmacology and Chemistry, Memorial Sloan-Kettering Cancer Center, 1275 York Avenue, New York, United States of America, NY10065.

Table of Contents

Materials and Methods

General details

All chemicals, unless otherwise stated, were purchase from SigmaAldrich (St. Louis, MO) and were used as received. Water (>18.2 MΩ·cm at 25 ºC, Milli-Q, Millipore, Billerica, MA) was purified by passing through a 10 cm column of chelex resin (Bio-Rad Laboratories, Hercules, CA) at a flow rate <1.0 mL/min. All instruments were calibrated and maintained in accordance with previously reported routine quality-control procedures.(*1*) Radioactivity measurements were made by using a Capintec CRC-15R Dose Calibrator (Capintec, Ramsey, NJ) with a calibration factor of 439, 015, 465, 570, 151 and 775×5 (at equilibrium) for ^{18}F, ^{64}Cu, ^{89}Zr, ^{124}I, ^{131}I and ^{225}Ac, respectively. For accurate quantification of radioactivities, experimental samples of positron-emitting radionuclides were counted for 1 min. on a calibrated Perkin Elmer (Waltham, MA) Automatic Wizard^2 Gamma Counter by using a dynamic energy window of 800–1000 keV for ^{89}Zr (909 keV emission). ^{89}Zr-radiolabeling reactions were monitored by using silica-gel impregnated glass-fibre instant thin-layer chromatography (ITLC-SG) paper (Pall Corp., East Hills, NY) and analyzed on a radio-TLC plate reader (Bioscan System 200 Imaging Scanner coupled to a Bioscan Autochanger 1000 (Bioscan Inc., Washington, DC, using Win-Scan Radio-TLC software version 2.2). Solvent systems included diethylene triamine pentaacetic acid in water (DTPA, 50 mM, pH7) and phosphate buffered saline (PBS). The LNCaP human prostate cancer cell line was obtained from the American Type Culture Collection (ATCC, Manassas, VA) and cells were grown by serial passage using standard methods.

Xenograft models

All animal experiments were conducted in compliance with Institutional Animal Care and Use Committee (IACUC) guidelines and the NIH Guide for the Care and Use of Laboratory Animals. All animal procedures were performed under anesthesia by inhalation of 1-2% isoflurane (Baxter Healthcare, Deerfield, IL)/oxygen mixture. After the studies, all animals were sacrificed by CO_2 asphyxiation. Male SCID mice (C.B-*Igh-1*^{b}/IcrTac-*Prkdc*^{scid}, 20–22 g, 4–6 weeks old) were obtained from Taconic Farms Inc. (Hudson, NY), and were allowed to acclimatize at the MSKCC vivarium for 1 week prior to implanting tumors. Mice were provided with food and water *ad libitum*. LNCaP tumors were induced on the right and left flank by sub-cutaneous (s.c.) injection of 4.0×10^{6} cells in a 100 μL cell suspension of a 1:1 v/v mixture of media with reconstituted basement membrane (BD Matrigel™, Collaborative Biomedical Products Inc., Bedford, MA). Palpable LNCaP tumors (50–250 mm^3) developed after a period of 4 weeks. The tumor volume (V / mm^3) was estimated using previously described methods.(*2*)

Acute biodistribution studies

Acute *in vivo* biodistribution studies were conducted at the end of the optical and immuno-PET imaging to validate the uptake and localization of ^{89}Zr-DFO-J591 observed in mice bearing dual s.c. LNCaP (50–250 mm^3) tumors (n=3). Full details are presented in the supporting information. Mice were anesthetized then sacrificed by CO_2 asphyxiation at 96 h post-administration. Eleven tissue samples were collected including the tumors, rinsed in water, dried in air for 5 min., weighed and subjected to optical imaging to generate the optical signal originating from each organ (*vide infra*). The organs were then stored at 4 ºC for 10 days to allow the activity to decay to a level suitable for counting on the gamma counter. Count data (counts per minute [c.p.m.]) were background- and decay-corrected before a standard calibration curve was used for the numerical conversion to activity (kBq). The percentage injected-dose-per-gram (%ID/g) for each tissue sample was then calculated by normalization to both the total amount of activity injected (kBq) and the organ mass (g).

PET imaging

PET imaging experiments were conducted on a microPET Focus 120 scanner (Concorde Microsystems) (*3*). PET images of the *in vitro* phantoms were recorded by using the same methods and instrument parameters as described for the small-animal immuno-PET studies.

Mice were administered ^{89}Zr-DFO-J591 formulations (10.9–11.3 MBq, [295–305 μCi], 60–62 μg of mAb, in 200 μL sterile saline for injection) *via* retro-orbital (r.o.) injection. Approximately 5 min. prior to recording PET images, mice were anesthetized by inhalation of 1-2% isoflurane/oxygen gas mixture and placed on the scanner bed. PET images were recorded at various time-points between 24–96 h post-injection. List-mode data were acquired for between 10 and 30 min. using a γ-ray energy window of 350–750 keV, and a coincidence timing window of 6 ns. For all static images, scan time was adjusted to ensure a minimum of 20 million coincident events were recorded. Data were sorted into 2-dimensional histograms by Fourier re-binning, and transverse images were reconstructed by filtered back-projection (FBP) into a 128×128×63 (0.72×0.72×1.3 mm) matrix. For the ^{89}Zr-DFO-J591 immuno-PET images the reconstructed spatial resolution for ^{89}Zr was 1.9 mm full-width half-maximum (FWHM) at the center of the field-of-view (FOV). The image data were normalized to correct for non-uniformity of response of the PET, dead-time count losses, positron branching ratio, and physical decay to the time of injection but no attenuation, scatter, or partial-volume averaging correction was applied. An empirically determined system calibration factor (in units of [mCi/mL]/[cps/voxel]) for mice was used to convert voxel count rates to activity concentrations. The resulting image data were then normalized to the administered activity to parameterize images in terms of %ID/g. Manually drawn 2-dimensional regions-of-interest (ROIs) or 3-dimensional volumes-of-interest (VOIs) were used to determined the average %ID/g (decay corrected to the time of

injection) in various tissues/phantom tubes. Images were analyzed by using ASIPro VM™ software (Concorde Microsystems).

Optical imaging

Optical images were acquired by using the Xenogen Ivis 200 optical imager. Cerenkov radiation was detected from each phantom containing various activities of the same radionuclide by using the bioluminescence setting (Integration time: 10, 20, 30, 40, 50, 60 s; , f/stop:1; binning 1, field of view B) with no light interference from the excitation lamp. Spectral analysis was obtained by measuring optical images either with or without the use of a narrow band filter (560, 580, 600, 620, 640 and 680, or open filter) with 20 nm full-width at half-maximum (FWHM) resolution.

Animals were anesthetized and imaged at 24, 48, 72, 96 h post-injection of ^{89}Zr-DFO-J591. Images were collected by using open filter for planar imaging and the narrow band filters for tridimensional reconstruction of data. Images were collected and analyzed by using the Living Image 3.6 and 2.6 software (Caliper Life Sciences, Alameda, CA), respectively. The average radiance (p/s/cm^2/sr) was used for quantitative region-of-interest (ROI) analysis from each image. Background correction was performed either through the use of dark images acquired at the equivalent instrument integration settings immediately before experimental image collection or by ROI analysis of a region in the same experimental image but remote from the area of interest.

J591 conjugation

Antibody conjugation and radiolabeling

The IgG_1 monoclonal antibody J591 was conjugated to the *tris*-hydroxamate, hexadentate chelate, desferrioxamine B (DFO, Calbiochem, Spring Valley, CA) by using a 6-step procedure modified(*2*) from that described by Verel *et al*.(*4*) Specific details of the chemistry are reported here as supporting information. Complete characterization of ^{89}Zr-DFO-J591 as a novel radiopharmaceutical for immuno-PET imaging of PSMA-positive prostate cancer *in vivo* will be reported elsewhere.

Synthesis of N-succinyldesferrioxamine B (N-succDFO)

DFO mesylate (0.508 g, 0.77 mmol, Calbiochem, Spring Valley, CA) was dissolved in pyridine (7.5 mL) and reacted with excess succinic anhydride (1.704 g, 0.017 mol) at room temperature for 24 h. The white suspension was then poured into NaOH(aq.) (120 mL, 0.015 mol dm^{-3}) and stirred at room temperature for 16 h. The colorless solution was adjusting to pH2 by the addition of 12 mol dm^{-3} HCl and cooled with stirring at 4 ºC for 2 h. The white precipitate was collected by filtration, washed with copious amounts of HCl (0.01 mol dm^{-3}) then water and dried *in vacuo* to give the *N*-succinyldesferrioxamine B (*N*-succDFO) as a white microcrystalline solid (0.306 g, 4.75×10^{-4} mol, 62%). HRMS-ES^+: Calc. for $[C_{29}H_{52}N_6O_{11} + H^+]$ = 661.3772; found 661.3760 ($[M + H^+]$ = 100%).

Preparation of [Fe(N-succDFO-TFP)] activated ester

N-succDFO (9.0 mg, 14 μmol) was suspended in 3.0 mL 0.9% sterile saline and the pH adjusted to 6.5 with 0.1 M Na_2CO_3(aq.) (50 – 75 μL in chelex purified water). Then a solution of $FeCl_3$•$6H_2O$ [4.0 mg, 15 μmol, 300 μL of 0.1 M HCl(aq.)] was added. Upon addition of the $FeCl_3$(aq.) the reaction mixture changes from colorless to deep orange due to the intense electronic absorption band of [Fe(DFO)] with a peak at 430 nm (ε_{430} = 2216 ± 49 mol^{-1} dm^3 cm^{-1}). After stirring the reaction at room temperature for 1 h, a solution of 2,3,5,6-tetrafluorophenol (TFP, 300 μL, 36 μmol, 1.2 mol dm^{-3} in chelex purified MeCN; SigmaAldrich, St. Louis, MO) was added to the reaction followed by addition of solid *N*-(3-dimethylaminopropyl)-*N'*-ethylcarbodiimide hydrochloride (EDAC, 120 mg, 0.63 mmol, SigmaAldrich). The reaction mixture (pH6.5) was then stirred at room temperature for 1 h before purifying the [Fe(*N*-succDFO-TFP)] product by use of a C-18 Light Sep-pak cartridge (Waters, Milford, MA). The reaction mixture was loaded onto a pre-activated (6 mL MeCN, 10 mL H_2O) C-18 cartridge, washed with copious amounts of water (>40 mL), and eluted with 1.5 mL MeCN. The final [Fe(*N*-succDFO-TFP)] solution had a concentration approximately 9.8 mM. The [Fe(*N*-succDFO-TFP)] solution can be stored for 24 h at 4 ºC but the most efficient conjugation reactions were achieved by using fresh preparations.

Preparation of DFO-J591

Humanized monoclonal antibody J591 (5 mg/mL, 1 mL, ~33 nmol, MW ~150,000 g mol^{-1}) was added to a centrifuge vial and the pH adjusted to 9.5 – 10.0 by using aliquots of 1.0 M and 0.1 M Na_2CO_3(aq.). Then 6 equivalents of [Fe(*N*-succDFO-TFP)] (200 nmol, 20 μL, 9.8 mM) was added and gently mixed using an automated pipette. The reaction was allowed to react at room

temperature without agitation for 1 h. Then 2,5-dihydroxybenzoic acid [gentisic acid, 50 μL, 0.65 mol dm^{-3} in 0.32 M Na_2CO_3(aq.)] was added to the reaction and the pH was adjusted to 3.9 – 4.2 by the addition of 5 to 10 μL aliquots of 0.25 M H_2SO_4(aq.). Then a 10-fold excess of ethylenediaminetetraacetic acid disodium salt with [$EDTA^{2-}.2Na^{+}$(aq.), 0.0674 mol dm^{-3}, 13.7 μmol, 30 μL] with respect to [Fe(*N*-succDFO-TFP)] was added. The reaction was incubated in a water bath at 38 ºC for 1 h during which time the solution changed from clear yellow to colorless. Subsequent purification led to colorless solutions which were found to have immunoreactive fractions >0.9. The DFO-J591 was purified by size-exclusion chromatography (Sephadex G-25 M, PD-10, >30 kDa, GE Healthcare; dead-volume = 2.5 mL, eluted with 200 μL fractions of 0.9% sterile saline).

Radiolabeling of DFO-J591

^{89}Zr-DFO-J591 was prepared by the complexation of [^{89}Zr]Zr-oxalate with DFO-J591. Typical radiolabeling reactions were conducted in accordance with the following procedure. Briefly, [^{89}Zr]Zr-oxalate (153.2 MBq, [4.14 mCi]) in 1.0 M oxalic acid (170 μL) was adjusted to pH7.7–8.1 with 1.0 M Na_2CO_3(aq.). CAUTION: Acid neutralization releases CO_2(g) and care should be taken to ensure that no radioactivity escapes the microcentrifuge vial. After CO_2(g) evolution ceased, DFO-J591 (250 μL, 2.1 mg/mL [0.525 mg of mAb], in 0.9% sterile saline) was added and the reaction was mixed gently by aspirating with a pipette. The reaction was incubated at room temperature for between 1–2 h and complexation progress was monitored with respect to time by ITLC (DTPA, 50 mM, pH7). After 1 h, crude radiolabeling yields and RCP was >95%. ^{89}Zr-DFO-J591 was purified by using either size-exclusion chromatography (Sephadex G-25 M, PD-10 column, >30 kDa, GE Healthcare; dead-volume = 2.5 mL, eluted with 200 μL fractions of

0.9% sterile saline) or spin-column centrifugation (4 mL total volume, >30 kDa, Amicon Ultra-4, Millipore, Billerica, MA; washed with 4×3 mL, 0.9% sterile saline). The radiochemical purity (RCP) of the final ^{89}Zr-DFO-J591 (67% radiochemical yield; formulation: pH5.5–6.0; <500 μL; 0.9% sterile saline) was measured by both radio-ITLC and analytical size-exclusion chromatography (loading <0.74 MBq [20 μCi], ca. 5–10 μL aliquots) and was found to be >99% in all preparations. The final radiochemical yield of the purified ^{89}Zr-DFO-J591 was 67% and the product was formulated in 0.9% sterile saline with RCP >99% and a specific-activity of 165.0 MBq/mg (4.47 mCi/mg) of mAb. The specific-activity obtained in these studies compares favorably with the previously reported specific-activities of other ^{89}Zr-radiolabeled mAbs.(*2, 5-11*)

In the ITLC experiment ^{89}Zr-DFO-J591 and [^{89}Zr]Zr-DFO remain at the baseline (R_f = 0.0), whereas $^{89}Zr^{4+}$(aq.) ions and [^{89}Zr]Zr-DTPA elute with the solvent front (R_f = 1.0). Figure 1 shows typical radio-ITLC chromatograms of the crude and purified ^{89}Zr-DFO-J591 and Figure 2 shows a typical elution profile for the purification of ^{89}Zr-DFO-J591 by using PD-10 size-exclusion chromatography.

Figure 1. Radio-ITLC

Typical radio-ITLC chromatograms of the crude (red) and purified (blue) ^{89}Zr-DFO-J591. Eluant: DTPA(aq.), 50 mM, pH7. The ^{89}Zr-DFO-J591 remains at the baseline (R_f = 0.0) and impurities run with the solvent front (R_f = 1.0).

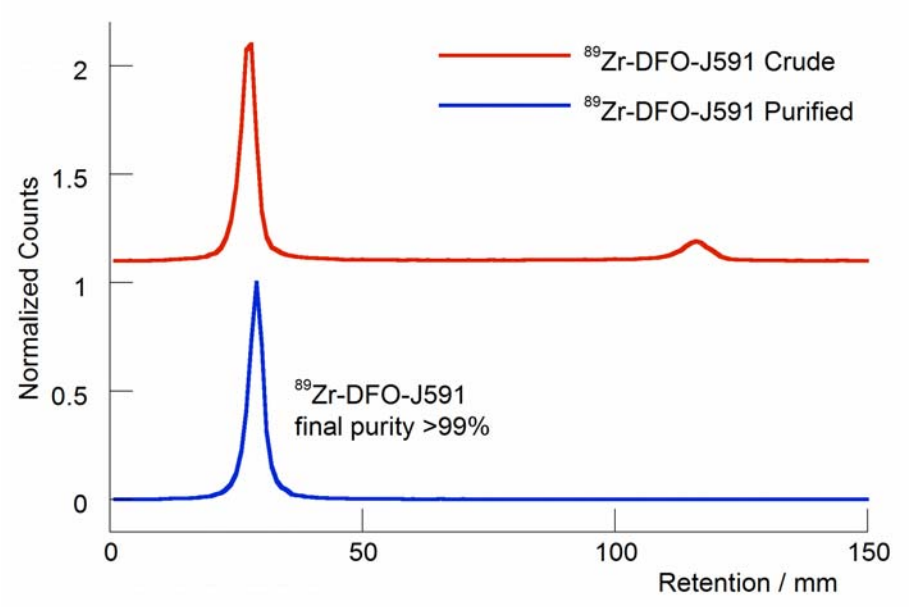

Figure 2. Size-exclusion chromatography

Typical elution profiles observed by using PD-10 size-exclusion chromatography for the purification of ^{89}Zr-DFO-J591 from small molecule (<30 kDa) ^{89}Zr-radiolabeled impurities and unreacted [^{89}Zr]Zr-oxalate (complexed as [^{89}Zr]Zr-DTPA). Species with molecular weights >30 kDa elute in the first 1.8 – 2.0 mL of solvent. NB: the first 2.5 mL dead volume was discarded prior to collecting the fractions.

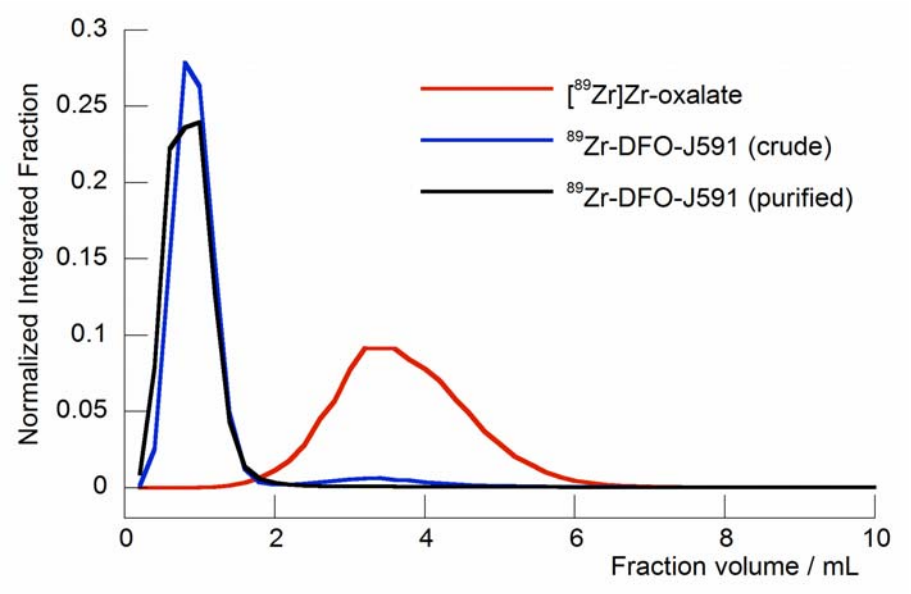

Chelate number

The number of accessible DFO chelates conjugated to J591 was measured by radiometric isotopic dilution assays following a method similar to that described by Anderson *et al*.(*12*) From a stock solution, aliquots of [^{89}Zr]Zr-oxalate (10 μL, 660 kBq [18 μCi], pH7.7–8.1 [pH adjusted using 1.0 M Na_2CO_3]) were added to 10 solutions containing 1:2 serial dilutions of non-radioactive $ZrCl_4$(aq.) (50 μL fractions; 250–0.5 pmol, pH7.7–8.1). The mixture was vortexed for 30 s before adding aliquots of DFO-J591 (5 μL, 2.1 mg/mL, [10.5 μg of mAb, 0.07 nmol], in 0.9% saline). The reactions were incubated at room temperature for 2 h before quenching with DTPA (20 μL, 50 mM, pH7). Control experiments confirmed that ^{89}Zr complexation to DFO-J591 was complete within <2 h. The extent of complexation was assessed by developing ITLC strips (DTPA, 50 mM) and counting the activity at the baseline and solvent front. The fraction of ^{89}Zr-radiolabeled mAb (A_b) was plotted *versus* the amount of non-radioactive $ZrCl_4$ added. The number of chelates was calculated by using linear regression analysis to calculate the concentration of $ZrCl_4$ at which only 50% of the DFO-J591 was labeled, multiplying by a factor of 2, and then dividing by the moles of mAb present in the reaction.

Isotopic dilution assays revealed an average of 3.9±0.3 accessible DFO chelates per mAb.

Immunoreactivity

The immunoreactive fraction of ^{89}Zr-DFO-J591 was determined by using specific radioactive cellular-binding assays following modified procedures derived from Lindmo *et al*.(*13, 14*) Briefly, LNCaP cells were suspended in micro-centrifuge tubes at concentrations of 5.0, 4.0, 3.0, 2.5, 2.0, 1.5, and 0.5 $\times 10^6$ cells/mL in 500 μL PBS (pH7.4). Aliquots (50 μL, <0.37 kBq, [<0.01 μCi]) of ^{89}Zr-DFO-J591 in 1% bovine serum albumin (BSA) were added to each tube (n = 3; final volume: 550 μL) and the samples were incubated on an orbital mixer for 60 min. at room temperature. Cells were then pelleted by centrifugation (600G for 2 min.), resuspended and washed twice with ice-cold PBS before removing the supernatant and counting the ^{89}Zr-radioactivity associated with the cell pellet. The count data were background corrected and compared with the total number of counts in control samples. Non-specific binding was assessed by using the same methods but with PC-3 (PSMA-negative) cells in place of LNCaP cells. Immunoreactive fractions were determined by linear regression analysis of a plot of (total/bound) activity *versus* (1/[normalized number of cells]), and calculated as 1/y-intercept.

The average immunoreactive fraction of ^{89}Zr-DFO-J591 was found to be 0.95±0.03 (n=4). Control experiments (n=4) using the PC-3 (PSMA-negative) cell line showed no binding which further demonstrated the specificity of ^{89}Zr-DFO-J591 for PSMA expressing cells.

Stability studies

The stability of ^{89}Zr-DFO-J591 with respect to change in radiochemical purity, loss of radioactivity from the mAb and/or change in immunoreactivity was investigated *in vitro* by incubation in solutions of 0.9% saline, and 1% BSA for 7 days at 37ºC. The radiochemical purity was determined by radio-ITLC and γ-counting, and the immunoreactive fraction was measured by using the LNCaP cellular-binding assay (*vide supra*).

Incubation of ^{89}Zr-DFO-J591 in either 0.9% saline or 1% BSA for 7 days at 37ºC revealed <2% decrease in RCP (*via* demetalation) with an observed ~17% decrease in the immunoreactive fraction for the 1% BSA experiment (0.78±0.03). Therefore, in the absence of specific proteolysis or reductive/oxidative metabolism, ^{89}Zr-DFO-J591 is expected to remain intact and immunoreactive *in vivo* on a time-scale suitable for immunoPET imaging.

Figure 3. *In vivo* optical image control

The figure shows the optical image of mice 1 – 3 acquired at 72 post-administration of ^{89}Zr-DFO-J591 both without (left) and with (right) a sheet of optically dense black paper placed over the mice. The picture confirms that the emission observed in the optical images is assigned to UV/vis light and is not an artifact due to interference of the γ-rays with the charge-coupled device (CCD) detector.

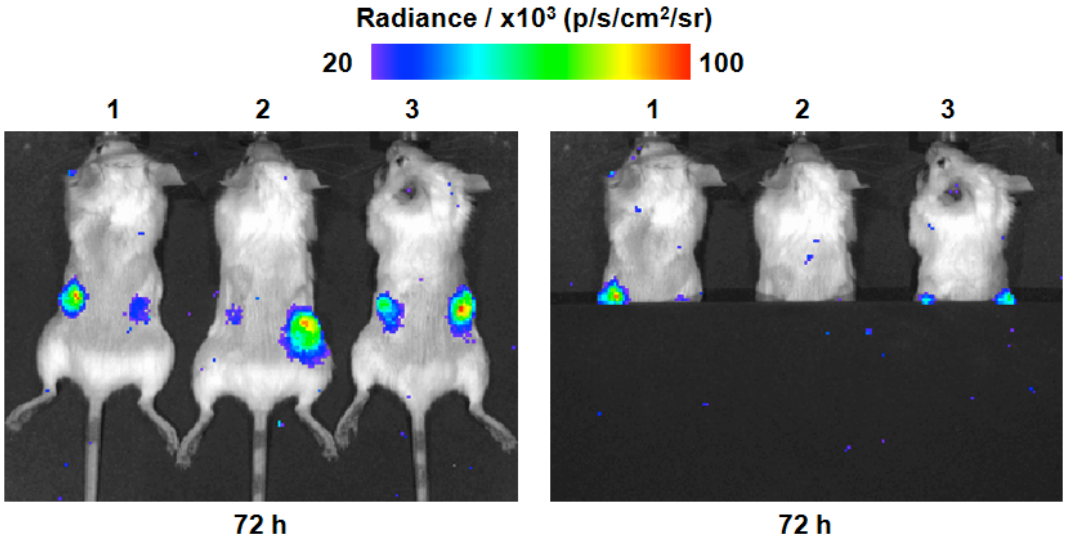

Figure 4. Time-activity curves

Time-activity curves (TACs) showing the region-of-interest (ROI) and volume-of-interest (VOI) analysis of (A) the CLI and (B) immuno-PET images for ^{89}Zr-DFO-J591 uptake in the well-established (large) LNCaP tumors. VOI analysis of the immuno-PET images showing the change in ^{89}Zr-activity in the heart/blood pool and muscle tissue is also presented.

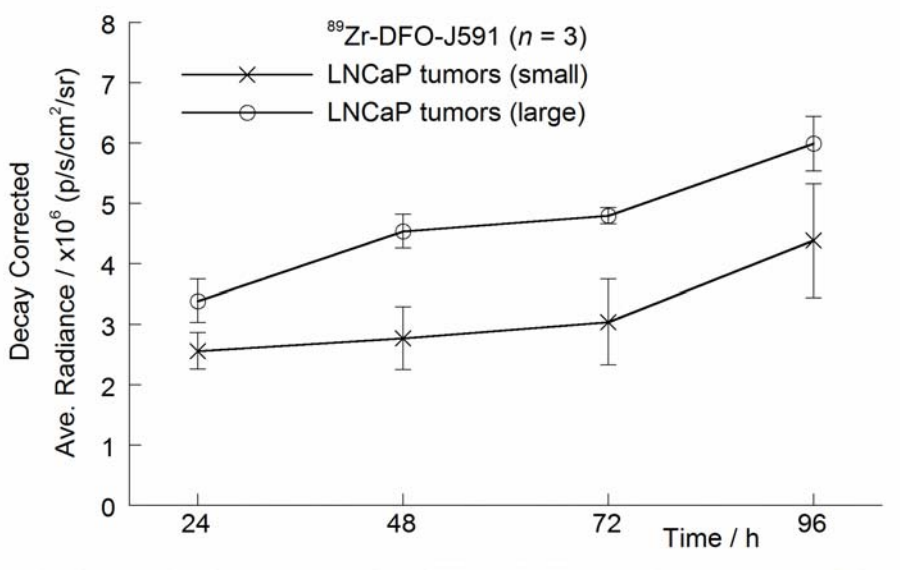

(A)

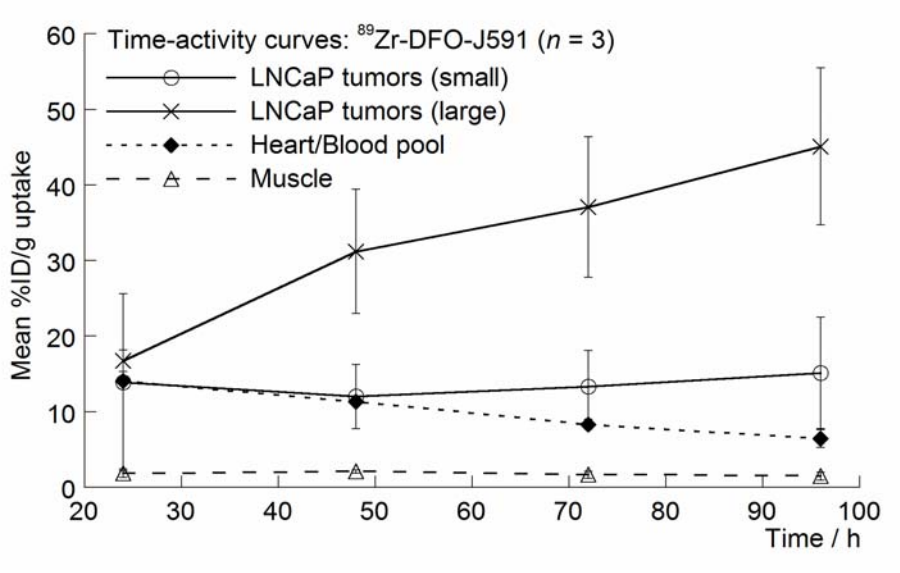

(B)

References

1. Zanzonico P. Routine quality control of clinical nuclear medicine instrumentation: a brief review. *J Nucl Med.* 2009;49(7):1114-1131.

2. Holland JP, Caldas-Lopes E, Divilov V, et al. Measuring the pharmacokinetic effects of a novel Hsp90 inhibitor on HER2/*neu* expression in mice using ^{89}Zr-DFO-trastuzumab. *PLoS ONE.* 2010;5(1):e8859.

3. Kim JS, Lee JS, Im KC, et al. Performance measurement of the microPET Focus 120 scanner. *J Nucl Med.* 2007;48(9):1527-1535.

4. Verel I, Visser GWM, Boellaard R, Stigter-van Walsum M, Snow GB, van Dongen GAMS. ^{89}Zr immuno-PET: Comprehensive Procedures for the production of ^{89}Zr-labeled monoclonal antibodies. *J Nucl Med.* 2003;44:1271-1281.

5. Verel I, Visser GWM, Boellaard R, et al. Quantitative ^{89}Zr immuno-PET for in vivo scouting of ^{90}Y-labeled monoclonal antibodies in Xenograft-bearing nude mice. *J Nucl Med.* 2003;44:1663-1670.

6. Perk LR, Visser OJ, Stigter-van Walsum M, et al. Preparation and evaluation of ^{89}Zr-Zevalin for monitoring of ^{90}Y-Zevalin biodistribution with positron emission tomography. *Eur J Nucl Med Mol Imaging.* 2006;33(11):1337-1345.

7. Börjesson PKE, Jauw YWS, Boellaard R, et al. Performance of immuno-Positron Emission Tomography with zirconium-89-labeled chimeric monoclonal antibody U36 in the detection of lymph node metastases in head and neck cancer patients. *Clin Cancer Res.* 2006;12(7):2133-2140.

8. Borjesson PKE, Jauw YWS, de Bree R, et al. Radiation dosimetry of ^{89}Zr-labeled chimeric monoclonal antibody U36 as used for immuno-PET in head and neck cancer patients. *J Nucl Med.* 2009:jnumed.109.065862.

9. Perk LR, Stigter-van Walsum M, Visser GWM, et al. Quantitative PET imaging of Met-expressing human cancer xenografts with ^{89}Zr-labelled monoclonal antibody DN30. *Eur J Nucl Med Mol Imaging.* 2008;35(10):1857-1867.

10. Aerts HJWL, Dubois L, Perk L, et al. Disparity between in vivo EGFR expression and ^{89}Zr-labeled cetuximab uptake assessed with PET. *J Nucl Med.* 2009;50(1):123-131.

11. Dijkers ECF, Kosterink JGW, Rademaker AP, et al. Development and characterization of clinical-grade ^{89}Zr-trastuzumab for HER2/neu immunoPET imaging. *J Nucl Med.* 2009;50(6):974-981.

12. Anderson CJ, Schwarz SW, Connett JM, et al. Preparation, biodistribution and dosimetry of copper-64-labeled anti-colorectal carcinoma monoclonal antibody fragments 1A3-F(ab')$_2$. *J Nucl Med.* 1995;36(5):850-858.

13. Lindmo T, Boven E, Cuttitta F, Fedorko J, Bunn PA, Jr. Determination of the immunoreactive fraction of radiolabeled monoclonal antibodies by linear extrapolation to binding at infinite antigen excess. *J Immunol Methods.* 1984;72(1):77-89.

14. Lindmo T, Bunn PA, Jr. Determination of the true immunoreactive fraction of monoclonal antibodies after radiolabeling. *Methods Enzymol.* 1986;121(Immunochem. Tech., Pt. I):678-691.